Magnetostratigraphic and archaeological records at the Early Pleistocene site complex of Madigou (Nihewan Basin): implications for human adaptations in North China

Shuwen Pei[a,b*], Chenglong Deng[c*], Ignacio de la Torre[d], Zhenxiu Jia[e], Dongdong Ma[a,b,f], Xiaoli Li[g], Xiaomin Wang[a,b]

[a] Key Laboratory of Vertebrate Evolution and Human Origins, Institute of Vertebrate Paleontology and Paleoanthropology, Chinese Academy of Sciences, Beijing 100044, China

[b] CAS Center for Excellence in Life and Paleoenvironment, Beijing 100044, China

[c] State Key Laboratory of Lithospheric Evolution, Institute of Geology and Geophysics, Chinese Academy of Sciences, Beijing 100029, China

[d] Institute of Archaeology, University College London, 31-34 Gordon Square, WC1H 0PY London, United Kingdom

[e] Institute of Tibetan Plateau Research, Chinese Academy of Sciences, Beijing 100101

[f] University of Chinese Academy of Sciences, Beijing 100049, China

[g] Beijing Museum of Natural History, Beijing 100050, China

[*]Corresponding author: peishuwen@ivpp.ac.cn (S. Pei),

cldeng@mail.iggcas.ac.cn (C. Deng)

ABSTRACT

The Nihewan Basin in North China contains the densest concentration of early Pleistocene Paleolithic sites outside Africa. This paper introduces a new archaeological site complex at Madigou (MDG) that was systematically excavated from 2011 to 2014 in the northeastern part of the Nihewan Basin. The site contains fossils and well-preserved stone artefacts in fluvio-lacustrine sediments. Our magneto- stratigraphic results situate the MDG sedimentary sequence in the early Brunhes normal chron and the late Matuyama reverse chron, including the Jaramillo normal subchron. The MDG artifact layers are positioned within the pre-Jaramillo Matuyama chron, with an estimated age of ca. 1.2 Ma, close to the onset of Mid-Pleistocene climate transition. The MDG core and flake technology includes bipolar flaking of siliceous dolomite cobbles, and freehand flaking of chert and brecciated chert block fragments. Mammalian fauna and pollen compositions indicate that the MDG hominins lived in an open habitat varying from lightly-wooded grassland to an ecosystem dominated by sparse steppe near the shore of the Nihewan paleolake. Our combined results in the fields of archaeology, paleontology, palynology and magnetochronology suggest that innovations in technological behavior may correlate with adaptations to high environmental variability during the start of Mid-Pleistocene climate transition.

Key words: Magnetostratigraphy; early human adaptations; Early Pleistocene; Madigou site complex; Nihewan Basin; North China

1. Introduction

Clarifying the precise age, geographic setting, and behavioral contexts of the earliest colonization of the Old World are central issues in the study of human evolution (Anton and Swisher, 2004; Zhu et al., 2003; Anton et al., 2014). The success of early human migrations from Africa into Asia has been predicated on a suite of morphological and behavioral adaptations to new environments and rapidly changing climatic conditions (Potts, 1996, 2012; Dennell and Roebroeks, 2005; Anton, 2007; Dennell, 2009, 2010; Klein, 2009; Braun et al., 2010; Norton and Braun, 2010; Henke and Hardt, 2011; Winder et al., 2015). The Nihewan Basin in North China, which contains the densest concentration of Early Pleistocene Paleolithic sites outside Africa, is a key area to explore early human evolution and behavior in East Asian northern latitudes following the earliest 'Out of Africa' (Schick et al., 1991; Zhu et al., 2001, 2004; Dennell, 2013).

The Nihewan Basin is located in the transition zone between the North China Plain and the Inner Mongolian Plateau (Fig.1a, b), and is filled with Pliocene to Holocene fluvio-lacustrine and aeolian deposits (Barbour, 1925; Barbour et al., 1927; Deng et al., 2008, 2019; Liu et al., 2018). It was initially best known for its long paleontological sequence (Teilhard de Chardin and Piveteau, 1930; Qiu, 2000; Cai et al., 2013), but numerous Early Pleistocene archaeological sites have been discovered since the 1970s as well (You et al., 1980; Wei and Xie, 1989; Xie et al., 2006). During the past decades, more than 60 Paleolithic sites associated with Mode 1 stone tools (i.e., core and flake assemblages) have been found in the basin

(Xie et al., 2006; Keates, 2010; Yuan et al., 2011; Liu et al., 2013), and a series of early sites have now been dated between the upper boundary of the Olduvai normal subchron and the Matuyama-Brunhes geomagnetic reversal (1.78–0.78 Ma) (e.g., Zhu et al., 2001, 2003, 2004; Wang et al., 2005; Deng et al., 2006b, 2007; Ao et al., 2010a, 2013a, b; Liu et al., 2010).

Current evidence shows that the Nihewan Basin was an area of consistent hominin occupation for a long span of ~1300 kyr, from ~1.7 to ~0.4 Ma (Zhu et al., 2001, 2004; Wang et al., 2005; Ao et al., 2010b, 2013a; Zuo et al., 2011). The number of sites, density of archeological remains within each site and their stratigraphic recurrence are in accord with an archaeological signal of hominins "settling in" rather than merely "passing through" (Potts and Teague, 2010), although convincing arguments have also been given to support a pattern of sporadic occupation (Dennell, 2013). Therefore, the question remains whether hominins with a Mode 1, core and flake technology could withstand the seasonal and longer-term oscillations in climate, and how hominins adapted their technological strategies during the Mid-Pleistocene climate transition (MPT) (ca. 1.25–0.7 Ma), characterized by high climate variability (Clark et al., 2006; Head et al., 2008; Head and Gibbard, 2015). To address these questions, large-scale archaeo-stratigraphic sequences with precise age determinations are vital to explore the hominin behavioral patterns and adaptations in the Nihewan Basin during MPT.

Madigou (MDG), a small gully of 400 m long and 20-40 m wide, is situated

940-1,000 m a.s.l. on the northwest margin of the Cenjiawan Platform (Barbour et al., 1927) at N40°13′07-16″, E114°39′58″-40′18″, and between the two well-known Early Paleolithic sites of Xiaochangliang and Donggutuo (Fig.1c). The MDG site was discovered in 1981 and was re-explored in 2007 (Pei et al., 2010), but systematic excavation was only conducted from 2011 to 2014, the results of which are presented here. In this paper, we present the MDG site complex archaeo-stratigraphic sequence, high-resolution magnetostratigraphic dating, archaeological assemblages, and discuss the significance of hominin technological behavior during the start of the MPT in the Nihewan Basin.

2. Geology and stratigraphy

2.1 Geology

The Nihewan Basin is an inter-montane down-faulted basin at the northeastern margin of the Chinese Loess Plateau (Fig. 1a, b). Late Pliocene to middle/late Pleistocene fluvio-lacustrine sediments were widely deposited in the basin (Young, 1950; Zhou et al., 1991; Zhu et al., 2003; Deng et al., 2008, 2019; Liu et al., 2012, 2018). The Nihewan Formation (Min and Chi, 2003) represents the type section of the Early Pleistocene in North China (Young, 1950), and is restricted to the lower part of the Nihewan Beds. Thick and continuous exposures of these fluvio-lacustrine sequences (without obvious tilting) are found mainly along the SW-NE trending Sanggan River and SE-NW trending Huliu River on the Cenjiawan Platform (Barbour et al., 1927) to the northeastern margin of the Nihewan Basin, covering an area of some 20 km^2 with a local elevation of >120 m

(Fig. 1b, c).

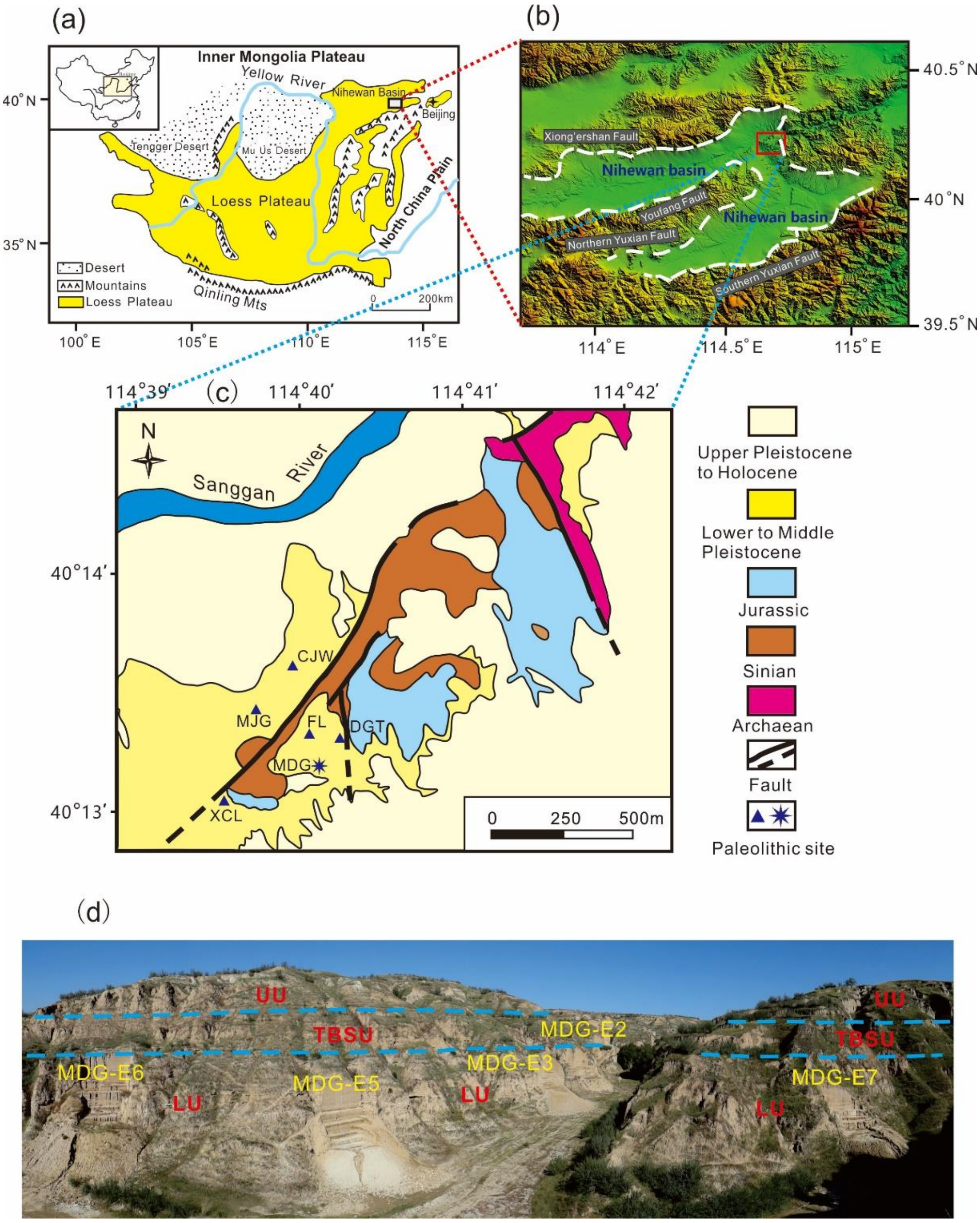

Fig. 1. Location of Madigou and its geological background. (a) Chinese Loess Plateau. (b) Sketch map of the Nihewan Basin. (c) relevant sites in the northeastern part of the Nihewan Basin. Upper Pleistocene to Holocene-loess/ paleosol/ alluvial deposits; Lower to Middle Pleistocene fine sand and silts;

Jurassic-volcanic lava and breccia; Sinian-siliceous dolomite with nodular or banded chert; Archaean-granulite and gneiss with banded quartz and quartzite. (d) Photo of the composite sections of MDG-E2, E3, E5, E6, and E7 at the MDG site complex (view from southwest); LU-lower unit, TBSU-thick brown sand unit, UU-upper unit.

2.2 Stratigraphy

The MDG site complex is located between the southern bank of the Sanggan River and the eastern bank of the Huliu River, around which several other Early Pleistocene Paleolithic sites are documented (Fig. 1c). In Madigou, the 44.1 m-thick Nihewan fluvio-lacustrine exposed deposits consist mainly of grayish-yellow and grayish-green silty clays, silts and sandy silts. Figure1d shows the lithostratigraphic profiles and position of the archaeological trenches at the MDG site complex. The lowest part of the MDG Section is the 16 m-thick Lower Unit (LU), which consists predominantly of massive sandy silts, silts, and pale gray silty clays. This unit shows horizontal and ripple beddings, and contains calcareous nodules and concretions, ferruginous nodules and rust spots, and complete and fragmentary mollusks. Above the LU is the Thick Brown Sand Unit (TBSU), with a thickness of 11.9 m and consisting of sands, silts, and clayey silts, all light brown in color. Thin horizontal lamination and ripple bedding are common. The next distinct unit is the Upper Unit (UU), which extends for 1.2 m in the reference section, and is formed of alternating light grey and light brown sand, silt, and clay. A dark gray clay that expands over 2 meters above the UU marks a well-developed weathering surface at the top of the Nihewan fluvio-lacustrine deposits. Loess sediments at the top of the section have been subjected to erosion, and are better preserved in some higher stratigraphic sections over the MDG sequence. Late middle to late Pleistocene tectonics and erosion shaped a west-east trending ravine of over 400 m in length. The MDG archaeological trenches are placed in the lake-margin silts and clays at 35.2–39.7 m from the top of the sequence, i.e. extending through sediments from the LU.

3 Methods

3.1 Rock magnetic measurements

To determine the magnetic mineralogy, four samples were selected for rock magnetic measurements, including temperature-dependent magnetic susceptibilities ($\chi-T$ curves), isothermal remanent magnetization (IRM) acquisition curves, backfield IRM demagnetization curves, and hysteresis loops (Fig. 2).

$\chi-T$ curves were measured using an AGICO MFK1-FA equipped with CS-3 temperature control system. Hysteresis loops, IRM acquisition, and back-field demagnetization curves were measured with a Princeton Measurements Corporation MicroMag 3900 vibrating sample magnetometer (VSM).

3.2 Paleomagnetic measurements

Block samples oriented by magnetic compass in the field were taken from four sub-sections, including MDG-E2, MDG-E3, MDG-E5 and MDG-E6. A total

629 block samples were taken at 10–20 cm intervals. Cubic specimens of 20×20×20 mm were obtained from those block samples in the laboratory.

Remanence measurements were made using a three-axis cryogenic magnetometer (2G Enterprises, USA) installed in a magnetically shielded space (<300 nT). To establish the magnetic polarity stratigraphy, 629 specimens were selected for paleomagnetic measurements. The specimens were subjected to progressive thermal or hybrid demagnetization. The thermally demagnetized specimens were subjected up to a maximum temperature of 690°C with 25–50°C interval below 585°C and 10–25°C above 585°C, using a Magnetic Measurements thermal demagnetizer with a residual magnetic field less than 10 nT. The hybrid-demagnetized specimens were subjected to 120°C thermal demagnetization followed by alternating field (AF) demagnetization at peak fields up to 70 mT. Both methods were capable of isolating the characteristic remanent magnetization (ChRM) after removal of soft secondary components of magnetization.

Demagnetization results (Fig. 3) were evaluated by orthogonal diagrams (Zijderveld, 1967) and the principal components direction was computed with the least-squares fitting technique (Kirschvink, 1980). The high-stability ChRM components were separated up to 585°C (Figs. 3a, 3h) or 680–690°C (Figs. 3b-3d, 3g, 3i), or up to 60–70 mT (Figs. 3e, 3f). The behaviors indicate that both magnetite and hematite dominate the remanence carriers in the MDG sediments. Total 261 (41.5%) specimens gave reliable ChRM directions. The maximum angular deviations (MAD) were usually smaller than 15°, with 3.8% of the 261 specimens having MAD values more than 15°. The virtual geomagnetic pole (VGP) latitudes were calculated from the ChRM data to construct the magnetostratigraphy for the MDG section (Figs. 4, 5).

3.3 Archaeological excavation and lithic analysis

Systematic mapping and geomorphological study of the MDG area was undertaken prior to excavations, focusing on the reference section of the fluvio-lacustrine deposits identified along the MDG small valley. All excavations were conducted in 2 to 5 cm spits, with larger spits used for sterile layers. Sediments were dry sieved with 5 mm mesh.

Stone tool analysis followed methodology outlined by Pei et al. (2017), which includes a consideration of basic technological categories of flaked, detached and pounded pieces, plus unmodified material (Isaac, 1986, Isaac et al., 1981; Pei et al., 2017; de la Torre and Mora, 2018).

4. Results

4.1 Rock magnetic measurements

Figure 2 shows the results of rock magnetic measurements. The $\chi-T$ curves (Figs. 2a-2d) are characterized by a major drop in magnetic susceptibility at ~585°C, the Curie point of magnetite, indicating that stoichiometric magnetite is the major contributor to magnetic susceptibility. Some samples display a clear susceptibility drop near 680°C (Figs. 2a, 2b, 2d), the Néel temperature of hematite, indicating that hematite contributed to the magnetic susceptibility. Some samples exhibit heating curves with a susceptibility hump near ~270–300°C (Figs. 2a, 2c, 2d). Further decrease of magnetic susceptibility between ~300°C and ~400°C is interpreted as the conversion of metastable maghemite (Stacey and Banerjee, 1974; Deng et al., 2006a). Cooling curves are higher than heating curves after exposure to <585°C. The significantly enhanced susceptibility after thermal treatment may arise from the neo-formation of magnetite grains from iron-containing silicates/clays (Deng et al., 2006a).

Analyzed samples display wasp-waisted hysteresis loops (Figs. 2e-2h), which are attributed to the coexistence of two magnetic components with strongly contrasting coercivities (Roberts et al., 1995). The low-coercivity component consists of magnetite and/or maghemite, and the high-coercivity component is mainly due to hematite. The open nature of the hysteresis loops up to fields of 1.0–1.5 T and the significantly low values of S-ratio (King and Channell, 1991), which is defined as the ratio of IRM acquired at –0.3 T ($IRM_{-0.3T}$) to IRM acquired at 1.5 T ($IRM_{1.5T}$), confirm the contribution of high-coercivity phases (e.g., Fig. 2j).

All samples show a rapid increase in the IRM acquisition curves below 100 mT (Figs. 2i-2l), indicative of the presence of magnetically soft components such as magnetite and maghemite. However, the IRM of all the selected samples continues to increase above 300 mT (Figs. 2i-2l), and the S-ratio has low values, suggesting a significant contribution from high-coercivity components, e.g., hematite (Fig. 2j).

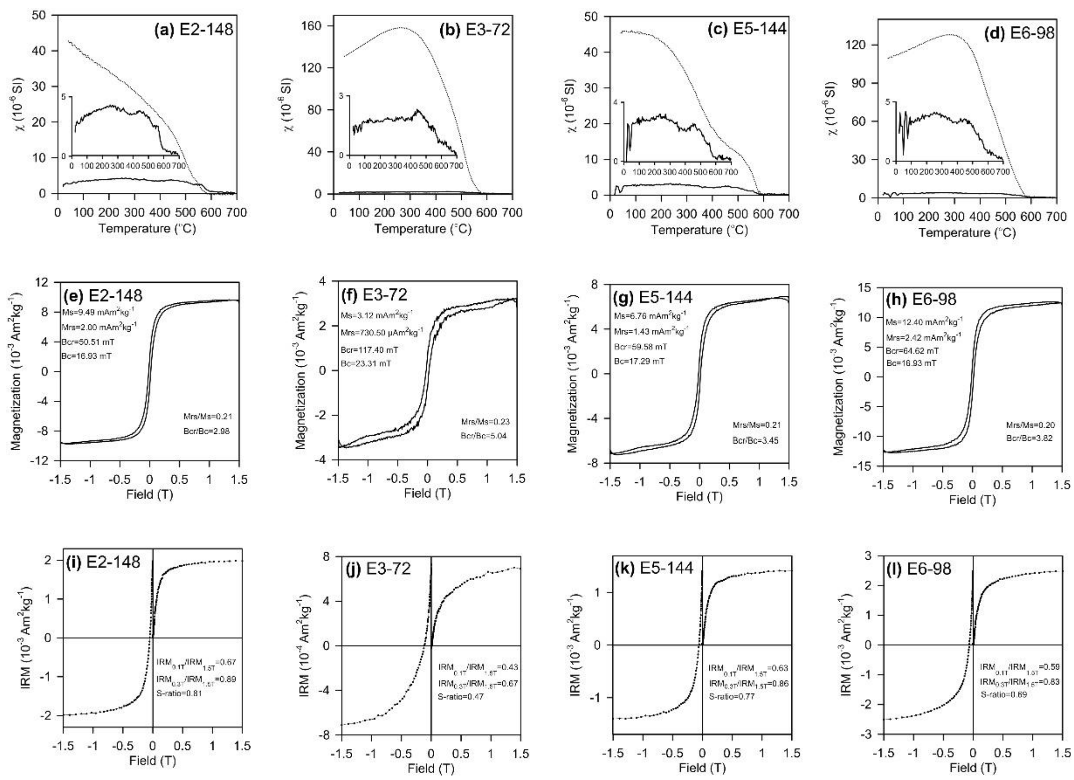

Fig. 2. Rock magnetic properties of representative samples. (a–d) Temperature-dependent magnetic susceptibilities (χ–T curves). Solid and dotted lines represent heating and cooling curves, respectively. (e–h) Hysteresis loops after high-field slope correction. Hysteresis parameters are indicated. (i–l) Isothermal remanent magnetization (IRM) acquisition curves and backfield demagnetization curves. Relevant magnetic parameters are indicated.

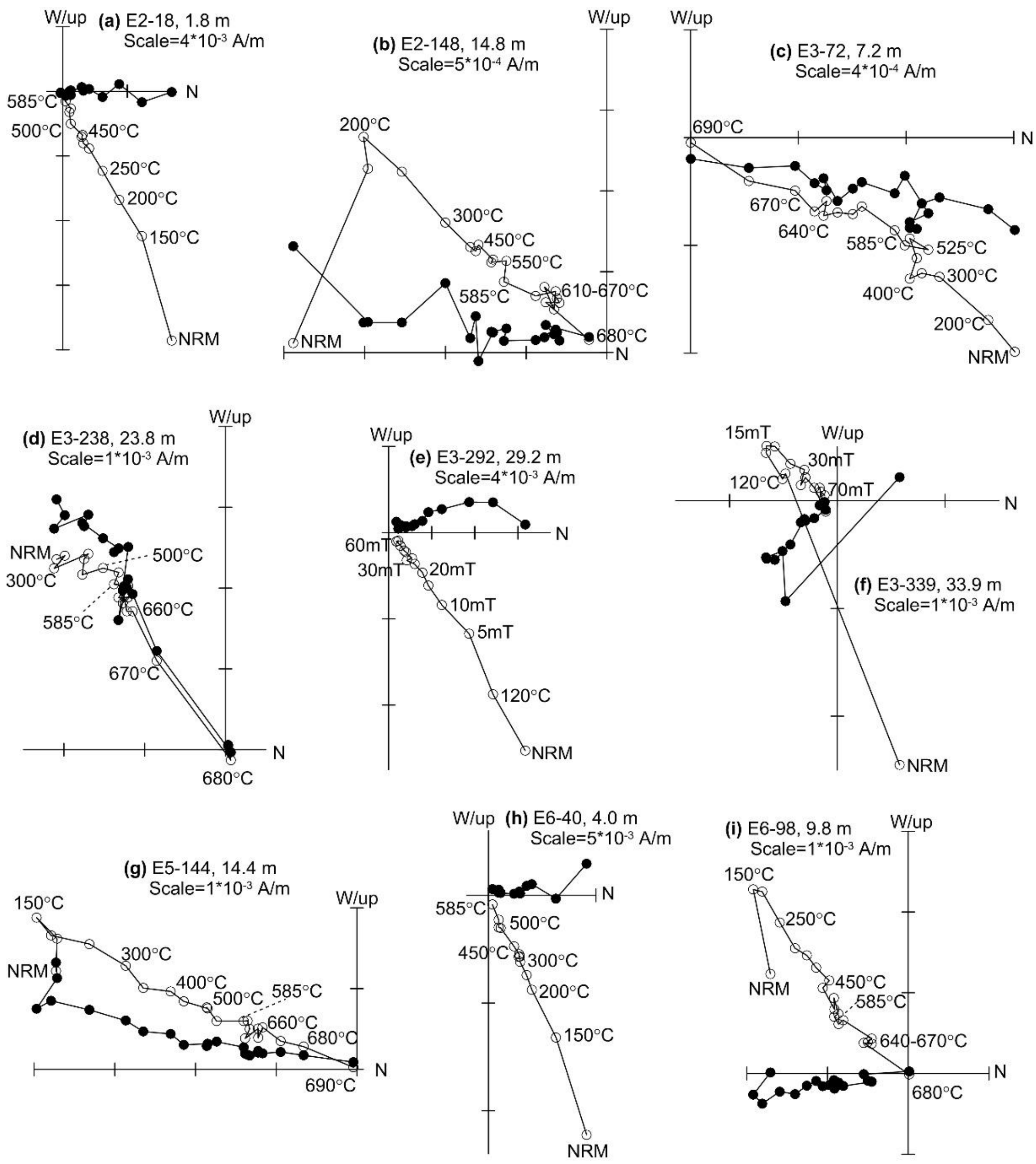

Fig. 3. Orthogonal projections of stepwise thermal and alternating field demagnetization data. The solid and open circles represent projections onto the horizontal and vertical plane, respectively. The numbers refer to temperatures in °C or alternating fields in mT. NRM is the natural remanent magnetization.

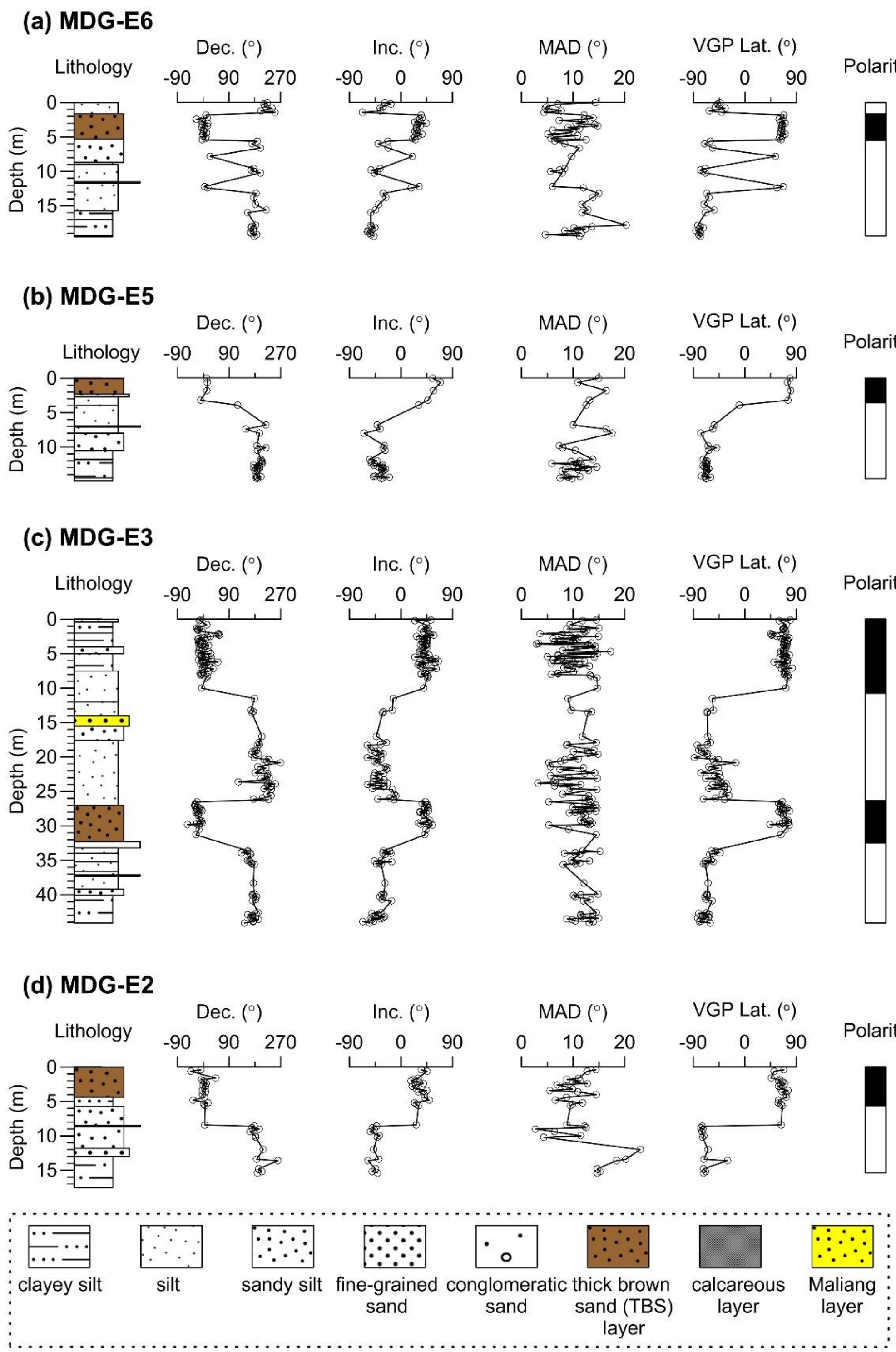

Fig. 4. Lithostratigraphy and paleomagnetic results of the four studied sub-sections. Dec., declination; Inc., inclination; MAD, maximum angular deviation; VGP Lat., latitude of virtual geomagnetic pole.

4.2 Stratigraphic correlation and age estimation of the Madigou site complex

The Madigou Paleolithic site is located ~150 m southwest of the Donggutuo and Huojiadi sites, and ~150 m southeast of the Feiliang site (Fig. 1c). The Donggutuo, Feiliang and Huojiadi sections mainly comprise fluvio-lacustrine silts, silty clays and sandy silts (Wang et al., 2005; Deng et al., 2007; Liu et al., 2010). A distinctive marker layer consisting of yellow sandy silts was used to stratigraphically correlate the Madigou section with the Donggutuo, Feiliang and Huojiadi sections. This marker layer (see position of the Maliang layer in Figures 4 and 5) which lies below the Matuyama-Brunhes boundary (Fig. 5) and can be traced in the field across several localities, is found at a depth interval of 14−15.5 m in the Madigou section (Fig. 5c), at 10−11 m depth in the Huojiadi section (Liu et al., 2010), 22.2–22.7 m depth in the Donggutuo section (Wang et al., 2005) and at 5.3−5.8 m depth in the Feiliang section (Deng et al., 2007).

Following demagnetization, four magnetozones are recognized within the Madigou section: two normal (N1 and N2) and two reverse (R1 and R2). The stone artifact layers occur within magnetozone R2.

Based on paleomagnetic and sedimentological data (Fig. 5), the Madigou magnetozones can be correlated with the astronomically-tuned Neogene timescale of Hilgen et al. (2012) (ATNTS2012). Magnetozones N1 and N2 correspond to the Brunhes normal chron and the Jaramillo normal subchron, respectively. Magnetozones R1 and R2 correspond to the pre- and post-Jaramillo Matuyama reverse chron, respectively.

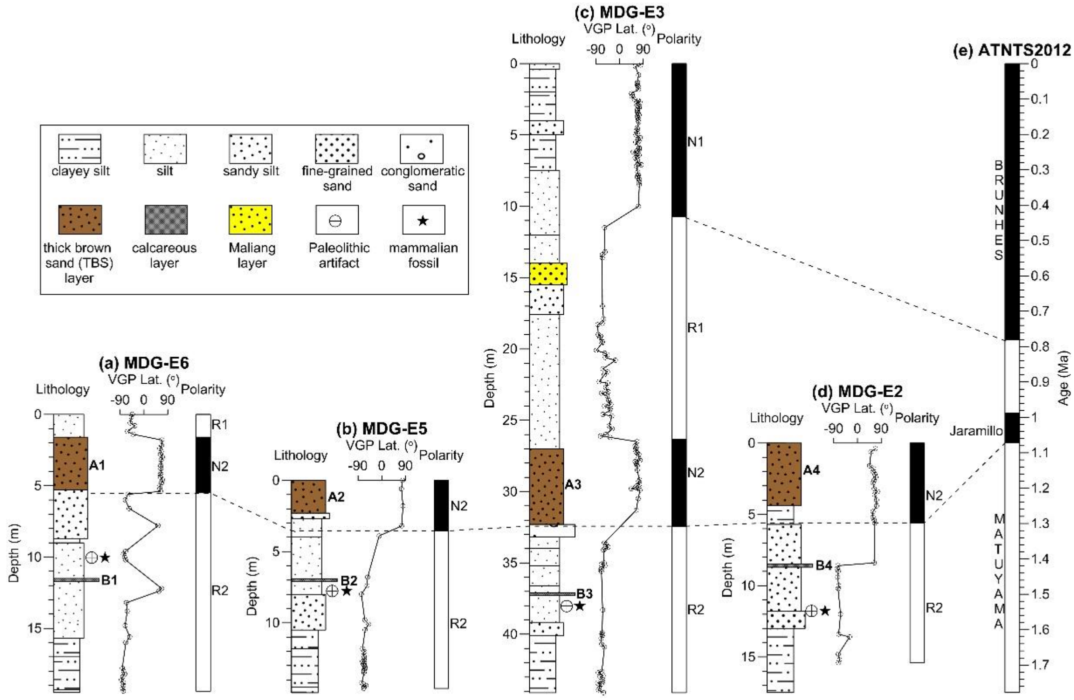

Fig. 5. Lithostratigraphy and magnetic polarity stratigraphy of the Madigou sub-sections MDG-E2, MDG-E3, MDG-E5 and MDG-E6, and their correlations with the astronomically-tuned Neogene timescale of Hilgen et al. (2012) (ATNTS2012). Layers A1−A4 and B1−B4 show the sedimentary marker layers used for local stratigraphic correlation.

The Madigou stone artifact layers occur just below the Jaramillo normal subchron, which was dated at 1.072−0.988 Ma in ATNTS2012 (Hilgen et al., 2012). We estimate the age of the Madigou artifact layer by extrapolating the sediment accumulation rate of MDG-E3 magnetozones R1−N2 (that is, between the Matuyama-Brunhes boundary and the lower boundary of the Jaramillo subchron) (Fig. 5). The average sediment accumulation rate of magnetozones

R1–N2 at MDG-E3 is 7.11 cm kyr^{-1}; hence, the extrapolated age estimate for the MDG-E3 stone artifact layer is 1.18 Ma. Given the significant variability in sediment accumulation rates among the fluvio-lacustrine sequences at MDG-E2, MDG-E3, MDG-E5 and MDG-E6, the age of the Madigou artifact layers is concluded to be around 1.2 Ma.

Importantly, two distinctive marker layers (namely A1–A4 and B1–B4) can be used for local stratigraphic correlation, further assisting to sequence the artifact layers of the Madigou sub-sections (Fig. 5). The marker layers A1–A4 consist of thick brown sand (TBS; named TBS layer) and are attributed to the Jaramillo interval. The marker layers B1–B4 consist of calcareous silts and sandy silts, which occur 2.9–6.0 m below the lower boundary of the Jaramillo subchron. Varying thickness of the Jaramillo and pre-Jaramillo sediments across the Madigou sub-sections is due to the high variability in sediment accumulation in the lake margin sequence.

The MDG-E3 and MDG-E5 artifact layers occur just below the marker layers B3 and B2 (Figs.5b and 5c), respectively, thus indicating the same age for both archaeological units. The MDG-E2 artifact layer occurs 3.1 m below the marker layer B4 (Fig. 5d), indicating that it is possibly older than the MDG-E3 and MDG-E5 artifact layers. The MDG-E6 artifact layer occurs 4.5 m below the lower boundary of the Jaramillo subchron and 1.5 m above the marker layers B1 (Fig. 5a). Considering these results, we propose a chronostratigraphic sequence for the early Pleistocene Madigou Paleolithic site complex that begins with MDG-E2, is followed by MDG-E3 and MDG-E5, and finishes with MDG-E6.

4.3 Archaeological assemblages

The excavation of five trenches (MDG-E2, MDG-E3, MDG-E5, MDG-E6， and MDG-E7) exposed a total area of 175 m^2 and more than 10 meters of the archaeo-stratigraphic sequence in the back walls. Archaeological remains, including 1517 stone tools and 900 fossil specimens, were unearthed from the lower part of the stratigraphy in each trench. Main features of each trench are available in Supplementary Information SI Table S1.

MDG bones are usually fragmentary. As shown in Table 1, the fossil assemblage includes *Equus* (represented mostly by isolated teeth), Rhinocerotide, *Gazella* and indeterminable bovids. The only rodent remain is a fragmentary skull with a well-preserved upper dentition, attributed to the genus *Spermophilus* (a typical ground squirrel). This faunal composition, dominated by grazers, indicates open grasslands and sparse steppe in the area.

Table 1 Taxonomic groups in the MDG fossil assemblage

Class	Taxon	Anatomical element	Environment
Perissodactyla	*Equus* sp.	Cheek teeth, metacarpal and tibia frag.	OG, SS
	Rhinocerotide gen. and sp. indet.	Cheek teeth and calcaneus frag.	OG
Artiodactyla	*Gazella* sp.	Cheek teeth and tibia frag.	OG, SS
	Bovidae gen. and sp. indet.	Phalange, tibia frag.	OG
Rodentia	*Spermophilus* sp.	Skull	OG, AS

Palaeoecological setting: OG=Open Grassland; AS= Arid Steppe; SS=Sparse Steppe

The lithic assemblage contains 1517 artefacts (Table 2) that weigh nearly 92 kg (frequency and weight of MDG stone tools per raw material is available in Supplementary Information SI Table S2). Most of the materials derive from MDG-E2 (n=857) and MDG-E3 (n=452), while the rest of trenches present low artefact densities (Table 2, also see the Supporting Information SI Table S1). Chert (n=679) is the most abundant raw material in terms of frequency of artefacts, followed by siliceous dolomite (n= 507) (see Supporting Information SI Table S2). Nonetheless, the latter is substantially more relevant (~42 kg) than chert (~24 kg) in terms of weight contribution to the assemblage, followed by brecciated chert and lava (see Supporting Information SI Table S2).

Numerically, detached artefacts (n=1194) dominate the assemblage, although the weight contribution of flaked pieces (~47 kg) is larger than that of detached pieces (~34 kg) (see Supporting Information SI Table S2, S3). Whole flakes (n=243) and flake fragments (n=385) are the most abundant categories and constitute 41.4% of detached artefacts (Table 2). Split cobbles are abundant (n=102), show clear anthropogenic signatures (e.g., clustered battering, bipolar damage, fresh fracture), and outnumber the frequency of cores (n=92) in the assemblage (Table 2).

Table 2 Breakdown of stone tool categories in the MDG site complex

Category		MDG-E2		MDG-E3		MDG-E5		MDG-E6		MDG-E7		Total	
		N	%	N	%	N	%	N	%	N	%	N	%
Detached	Flake	151	17.6	62	13.7	11	17.2	14	22.2	5	6.2	243	16.0
	Flake fragment	217	25.3	131	29.0	4	6.3	10	15.9	23	28.4	385	25.4
	Bipolar product	52	6.1	15	3.3	2	3.1	1	1.6	19	23.5	89	5.9
	Angular fragment<20mm	122	14.2	24	5.3	0	0.0	0	0.0	3	3.7	149	9.8
	Angular fragment>20mm	171	20.0	122	27.0	15	23.4	8	12.7	12	14.8	328	21.6
	Total Detached	713	83.2	354	78.3	32	50.0	33	52.4	62	76.5	1194	78.7
Flaked	Core	38	4.4	16	3.5	18	28.1	16	25.4	4	4.9	92	6.0
	Core fragment	3	0.4	9	2.0	1	1.6	2	3.2	0		15	1.0
	Retouched piece	52	6.1	13	2.9	8	12.5	2	3.2	1	1.2	76	5.0
	Bipolar core	13	1.5	4	0.9	1	1.6	2	3.2	2	2.5	22	1.5
	Split cobble	34	4.0	52	11.5	3	4.6	3	4.7	10	12.3	102	6.7
	Total Flaked	140	16.4	94	20.8	31	48.4	25	39.7	17	21.0	307	20.2
Pounded	Anvil	2	0.2	0		0		0		0		2	0.1
	Hammerstone	2	0.2	4	0.9	1	1.6	5	7.9	2	2.5	14	1.0
	Total Pounded	4	0.4	4	0.9	1	1.6	5	7.9	2	2.5	16	1.1
Grand total		**857**	**56.5**	**452**	**29.8**	**64**	**4.2**	**63**	**4.2**	**81**	**5.3**	**1517**	**100**

The MDG technology is geared towards the production of flakes of 3-4 cm in size using freehand and bipolar knapping techniques (Figs. 6j-m). Freehand cores are relatively small (74.6 mm of average length) and irregular, show short reduction sequences, and do not suggest standardized flaking methods (Figs. 6a-d). Cores and debitage bearing bipolar features are relatively abundant (see Table 2) which, added to the significant number of split cobbles [although see de la Torre and Mora (2018) for alternative interpretations of this category], indicate a great emphasis on the use of hammer-and-anvil techniques to knap stone tools. As shown in Supporting Information SI Table S2, there is a strong preference for the use of siliceous dolomite to produce split cobbles (see also Figs. 6e-i).

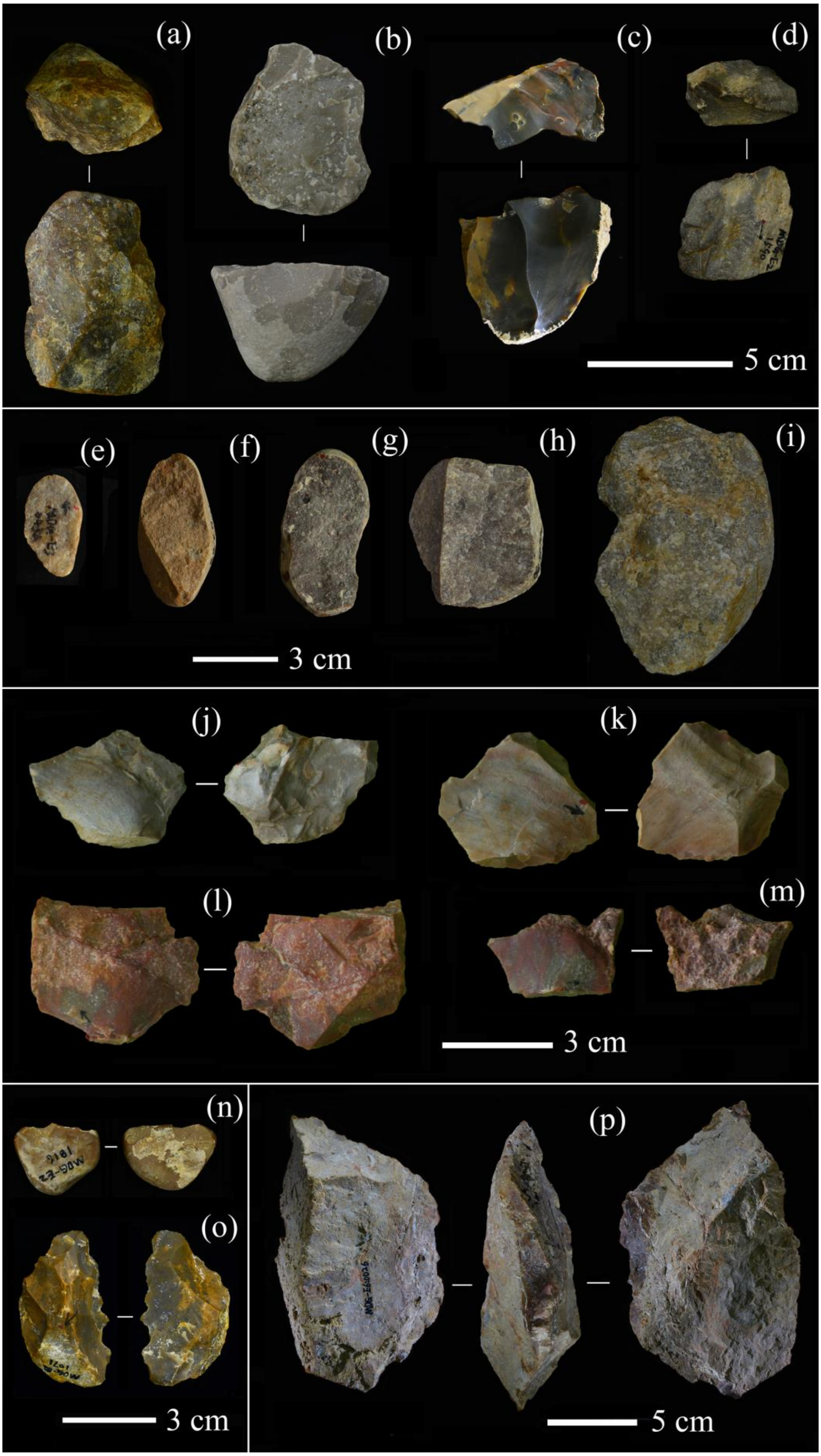
(a)
(b)
(c)
(d)
5 cm
(e)
(f)
(g)
(h)
(i)
3 cm
(j)
(k)
(l)
(m)
3 cm
(n)
(o)
3 cm
(p)
5 cm

Fig. 6. Stone tools from the MDG site complex

(a–d) cores, (e–i) split cobbles, (j–m) flakes, (n–o) small retouched tools, (p) large shaped tool.

Whilst MDG is essentially a core-and-flake assemblage, there is a significant number of finely retouched tools, predominantly of chert (see Supporting Information SI Table S2). Retouched tools are small in average (mm of mean length = 37.4 mm) and are usually made on flake blanks, although some retouched artifacts are made on small cobbles (Fig. 6m); convergent, point-shaping retouch is frequent (Fig. 6o). Two of these retouched artifacts surpass the 10 cm arbitrary cutoff (Kleindienst, 1962) for shaped pieces to be considered as Large Cutting Tools (LCTs) (Fig. 6p).

5. Discussion

5.1 Implications for hominin colonization of the northern high latitudes in East Asia

Early human evolution is significantly influenced by climate and environmental changes (Potts, 1996; Antón, 2007; Abbate and Sagri, 2012). The MPT was marked by a progressive increase in the amplitude of climate oscillations from 41 to 100 kyr cycles, which largely reflects combined changes in global ice volume, sea level, and ocean temperature (Ruddiman et al., 1986; Mudelsee and Schulz, 1997; Raymo, et al., 1997, Medina-Elizalde and Lea, 2005; Clark et al., 2006) (also see Fig. 7). This variability was accompanied by a series of paleoenvironmental processes of global or regional significance, such as rises in aridity and monsoonal intensity in Asia and Africa during the increased amplitude of climatic oscillations (Clark et al., 2006; Sun et al., 2019). Current evidence indicates that the earliest hominin populations to reach cold northeast Asia were able to survive for at least 0.5 myr prior to the MPT of high amplitude climate oscillations (Zhu et al., 2004) (Fig. 7). The environmental shifts in northern and northwestern China (An et al., 2005; Ding et al., 2005; Ao et al., 2012), which serve as habitat episodic disturbances, may have provided stress for early human evolution in this region, especially in the Nihewan Basin (Deng et al., 2006).

The MPT, previously known as the mid-Pleistocene Revolution (Maasch, 1988; Berger and Jansen, 1994; Mudelsee and Schulz, 1997), was marked by a progressive increase in the amplitude of climate oscillations (Ruddiman et al., 1986; Mudelsee and Schulz, 1997; Clark et al., 2006). Current evidence indicates that the MPT represents a critical phase in the evolution and dispersal of early *Homo* (Larick and Ciochon, 1996; Abbate and Sagri, 2012). During the earliest dispersal, hominins may have occupied Chinese Loess Plateau by 2.11 Ma (Zhu et al., 2018), were certainly present as far north as Dmanisi in Georgia by ~1.78-1.85 Ma (Gabunia and Vekua, 1995; Gabunia et al., 2000; Ferring et al., 2011), with sparse early records across the lower latitudes of central and tropical eastern Asia and southeastern Asia and subtropical southern China at around 1.7−1.6 Ma (Antón and Swisher, 2004; Dennell and Roebroeks, 2005; Zhu et al., 2008). By about 1.7−1.5 Ma, early *Homo* had definitely colonized the southern Loess Plateau in central China (Zhu et al., 2015) and the Nihewan Basin at high northern latitudes (40°N) (Zhu et al., 2004; Ao et al., 2013b). In East Asia, a population increase and geographic expansion from middle to high northern latitudes is observed at the onset of MPT (Larick and Ciochon, 1996; Deng et al., 2007; Abbate and Sagri, 2012). Our magnetochronological findings at the MDG Paleolithic site complex further document an unambiguous presence of early hominins during the MPT interval in the Nihewan Basin, previously supported by the evidence in Feiliang at ~1.2 Ma (Deng et al., 2007), Donggutuo (Wang et al., 2005) and Cenjiawan (Wang et al., 2006) at ~1.1 Ma, Huojiadi at ~1.0 Ma (Liu et al., 2010), and Maliang at 0.8 Ma (Wang et al., 2005).

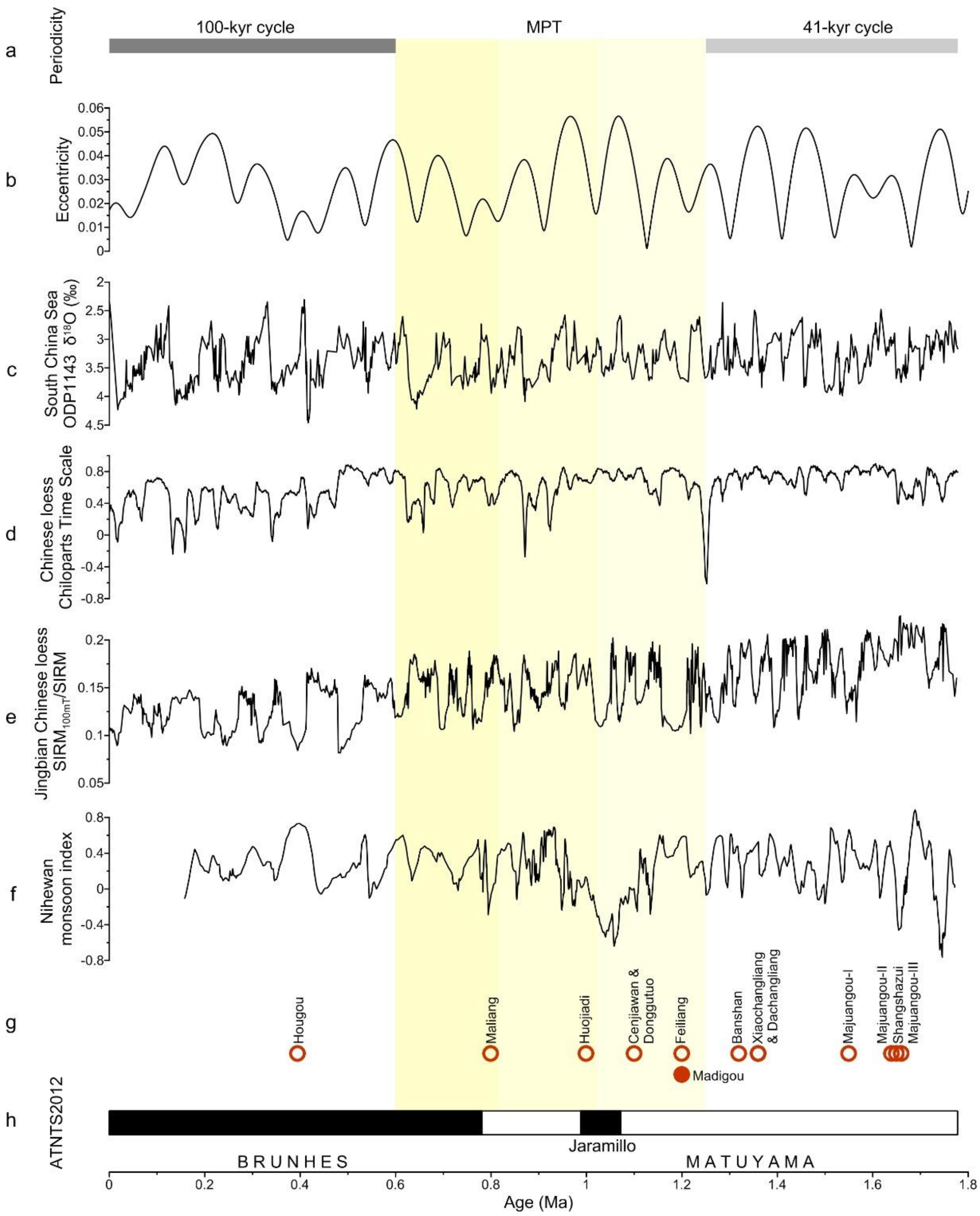

Fig. 7. Synthesis of well-dated early Paleolithic sites in the Nihewan Basin with respect to ATNTS2012 (Hilgen et al., 2012), and temporal variations of both marine and terrestrial paleoclimatic proxies in East Asia. (a) Paleoclimatic periodicities. (b) Long-term variations of eccentricity (Berger and Loutre, 1991). (c) $\delta^{18}O$ record from ODP Site 1143, South China Sea (Tian et al., 2002). (d)

Chinese loess Chiloparts time scale, which is the stacked grain-size age model for Chinese loess/paleosol sequences (Ding et al., 2002). (e) Changes in the $SIRM_{100mT}$/SIRM ratio from the Jingbian loess/paleosol sequence (SIRM is the saturation isothermal remanent magnetization, and $SIRM_{100mT}$ represents the residual SIRM after 100-mT alternating field demagnetization) (Deng et al., 2006a). (f) Tuned summer monsoon index of the Xiaodukou fluvio-lacustrine sedimentary sequence in the Nihewan Basin (Ao et al., 2012). (g) early Paleolithic sites in the Nihewan Basin. (h) ATNTS2012 (Hilgen et al., 2012). The shaded area represents the Mid-Pleistocene climate transition (MPT) (1.25−0.6 Ma) (Clark et al., 2006; Mudelsee and Schulz, 1997; Medina-Elizalde and Lea, 2005).

5.2 MDG contributes to extent the knowledge of early Paleolithic technological variability

The early Pleistocene archaeological evidence suggests that making and using stone artifacts was a regular part of early humans' subsistence strategies in the Nihewan Basin (Shen and Chen, 2003; Shen and Wei, 2004; Gao et al., 2005 Dennell, 2009; Keates, 2010; Liu et al., 2013; Guan et al., 2016; Yang et al., 2016, 2017). Chinese early stone tool assemblages have been traditionally attributed to a Mode 1, core-and-flake technology, which apparently underwent no significant innovations until the second part of the Late Pleistocene (Schick et al., 1991; Schick and Dong, 1993; Gao and Norton, 2002; Xie et al., 2006; Braun et al., 2010; Keates, 2000). In our recent review of the Nihewan early Pleistocene archaeological sequence (Pei et al., 2017), we have highlighted the expediency of core flaking methods and predominance of informal artifacts among retouched tools. However, Pei et al. (2017) and Yang et al. (2017) have both suggested that some variability may have existed in post-1.3~1.1 Ma assemblages, which is relevant to the present paper.

With regards to raw material procurement, there is consensus that early Pleistocene Nihewan hominins did not generally select higher-quality raw materials (Chen et al., 1999; Li, 1999; Shen and Chen, 2003; Keates, 2010). Instead, they collected locally ubiquitous poor-quality chert, which explains why most assemblages are characterized by very high frequencies of angular fragments, short reduction sequences, and low standardization of flaking schemes (Yang et al., 2016; Pei et al., 2017). Despite prevalence of this pattern, Shen and Wei (2004) observed that Maliang (0.8 Ma) and Cenjiawan (1.1 Ma) hominins might have preferentially selected good-quality raw materials, and Pei et al. (2017) reported that hominins at Feiliang (1.2 Ma) procured some fine-grained, high-quality chert, lava, and quartz. In the case of the MDG assemblage discussed here, a clear preference for some particular raw materials is observed: hominins used preferentially siliceous dolomite cobbles for bipolar flaking (Fig. 6g, 6h, and 6i), favored chert and brecciated chert block fragments for freehand flaking (Figs. 6j, 6k, 6l, and 6m), and selected high-quality chert for retouched tools (Figs. 6c and 6o).

As far as flaking techniques are concerned, the Nihewan Basin assemblages show that dominance of freehand expedient technologies was accompanied by variable frequencies of bipolar artefacts during the Early Pleistocene (Chen et al., 1999; Keates, 2000, 2010; Yang et al., 2016). Yang et al. (2017) see indications of novel flaking methods at Donggutuo (1.1 Ma), where they observe the use of freehand hard hammer percussion to pre-determine core shapes. At Cenjiawan, stone tool refitting indicates multidirectional flaking methods and continuous rotation of cores (Xie et al., 1994; Guan et al., 2016, Yang et al., 2017). Whilst MDG flaking techniques are majorly expedient, a more intensive reduction is observed in cores of good quality chert and dolomite (Figs. 3b and 3c), again suggesting raw material selectivity but also occasional use of recurrent flaking methods.

Proportions of retouched pieces in the Nihewan early Pleistocene lithic assemblages vary greatly, from less than 5% to more than 20% (Pei et al., 2017). Although often poorly standardized, morpho-types such as scrapers, notches, points, and denticulates have been described throughout the sequence (Wei, 1985; Xie et al., 1994; Guan et al., 2016; Yang et al., 2017; Pei et al., 2017; Liu et al., 2018). Despite yielding a lower proportion (5.0%) of retouched tools than the average in the Nihewan Early Pleistocene sequence, MDG shows that some elaborated retouched tools were manufactured in high quality raw materials (Figs. 6n and 6o), even if many still were relatively unstandardized. It is also relevant to comment on the size of retouched tools; the overwhelming predominance of small-sized flakes and retouched tools in the Nihewan assemblages is often attributed to poor quality of local raw materials, which render production of large blanks difficult (Yang et al., 2017). Nonetheless, evidence for core rotation and bifacial working of small clasts across some of the Nihewan assemblages indicate that hominins had the ability to fashion bifacial implements and, potentially, LCTs. In fact, two retouched artefacts from the MDG assemblage (Fig. 6p) exceed the >10 cm arbitrary cut-off often used to define LCTs, which might open new paths for the discussion on the reasons for their paucity in the Chinese sequence (Schick, 1994).

Overall, the MDG lithic assemblage contributes to highlight the variability of technological strategies across the Nihewan Basin sites, and to challenge the notion that the Mode 1, core-and-flake technology that characterize the Chinese early Pleistocene record was a homogeneous and static entity through time. Our results in MDG show that by ~1.2 Ma, there was a higher emphasis on bipolar flaking, strong raw material preference in flaking techniques and retouched tools, and that knappers possessed the ability to shape large tools, even when these are not the most characteristic artifacts in the assemblages.

It is still unclear to what extent techno-typological differences between MDG and other Nihewan early Pleistocene sites can be explained by palaeoecological and palaeogeographical constraints. Multiple lines of evidence at MDG show that the environment varied from a lightly-wooded grassland to an open semi-arid sparse steppe habitat with seasonally wet climate, and intermittent laminar flow control on the lake margin system (Li et al., 2016). The MDG bone assemblage responds to a steppe fauna adapted to the dry open grasslands. Increased palaeoecological variability associated with the onset of the MPT may have played a role in the affordances available to hominins, and may have contributed to the appearance of novel technological responses to the new climatic challenges.

Future research should place such hominin adaptations across the Nihewan Basin in a global perspective. Climate instability at the onset of the MPT might be responsible for technological variability in East African contexts (e.g., Potts, 1998, 2001), and could also potentially explain significant toolkit differences during the earliest colonization of western Europe (e.g., Parfitt et al., 2010; Vallverdu et al., 2014). By combining results across the Old-World record, we may be able to achieve a better understanding of how technological and biological plasticity enabled humans to adapt to variable and rapidly-changing conditions during one of the most challenging climatic periods of hominin evolution.

6. Conclusions

(1) Magnetostratigraphic results situate the Madigou sedimentary sequence in the early Brunhes normal chron and the late Matuyama reverse chron, including the Jaramillo normal subchron. Stratigraphic correlations of lithological and magnetic polarity sequences between the Madigou, Feiliang, Donggutuo and Huojiadi sections indicate that the Madigou artifact layers are contained within the pre-Jaramillo Matuyama chron. The age of the Madigou Paleolithic site complex is estimated to be ca. 1.2 Ma.

(2) The MDG assemblage contains fossils of several mammal species, including *Equus*, Rhinocerotide, *Gazella* and indeterminable bovids. The lithic assemblage is

typical of a Mode 1, core-and-flake technology. Like other Old World Mode 1 assemblages, the MDG stone industry is characterized by a simple technological design, low degree of standardization, expedient flaking, and a few non-standardized retouched flakes. The MDG core and flake technology includes bipolar flaking of siliceous dolomite cobbles, and freehand flaking of chert and brecciated chert block fragments. Knappers intentionally selected good-quality raw materials to manufacture small flakes and finely-retouched tools.

(3) Mammalian faunal and pollen compositions indicate that the MDG hominins lived in an open habitat varying from lightly-wooded grassland to an ecosystem dominated by sparse steppe near the shore of the Nihewan paleolake.

Overall, our findings suggest that the increased variability associated to the onset of the MPT may have played a role in the affordances available to hominins, and may have contributed to the appearance of novel technological responses to the new climatic challenges.

Acknowledgements

We would like to thank Mohamed Sahnouni, Sileshi Semaw, Kathy Schick, and Nicholas Toth for discussions and comments. We also thank Dr. Y. Guan and D. W. Niu for their help during the field work and Dr. Q. Li for identifying the microfauna specimen. Further thanks are due to the officials and antiquities personnel of the Hebei province and the local governments in Yangyuan County who facilitated fieldwork. Paleomagnetic and mineral magnetic measurements were made in the Paleomagnetism and Geochronology Laboratory, Institute of Geology and Geophysics, Chinese Academy of Sciences. This research was supported by the Strategic Priority Research Program of Chinese Academy of Sciences (Gran No. XDB26000000), the National Natural Science Foundation of China (41872029, 41804066, 41372032, 41690112), the Chinese Academy of Sciences President's International Fellowship Initiative (Grant No. 2017VCA0038), and the John Templeton Foundation through a grant to the Stone Age Institute.

References

Abbate, E., Sagri, M., 2012. Early to Middle Pleistocene Homo dispersals from Africa to Eurasia: Geological, climatic and environmental constraints. Quat. Int. 267: 3-19.

An, Z. S., Huang, Y. S., Liu, W. G., Guo, Z. T., Steven, C., Li, L., Warren, P., Ning, Y. F., Cai, Y. J., Zhou, W. J., Lin, B. H., Zhang, Q. L., Cao, Y. N., Qiang, X. K., Chang, H., Wu, Z. K., 2005. Multiple expansions of C_4 plant biomass in East Asia since 7 Ma coupled with strengthened monsoon circulation. Geology 9(33), 705–708.

Antón, S. C., 2007. Climatic influences on the evolution of early *Homo*? Folia. Primatol. 78, 365-388.

Antón, S. C., Potts, R., Aiello L. C., 2014. Evolution of *Homo*: An integrated biological perspective. Science 345(6192):1236828(1-13).

Antón, S.C., Swisher, C.C., 2004. Early dispersals of Homo from Africa. Annu.

Rev. Anthropol. 33, 271- 296.

Ao, H., An, Z.S., Dekkers, M.J., Li, Y.X., Xiao, G.Q., Zhao, H., Qiang, X.K., 2013a. Pleistocene magnetochronology of the fauna and Paleolithic sites in the Nihewan Basin: Significance for environmental and hominin evolution in North China. Quat. Geochronol. 18, 78-92.

Ao, H., Dekkers, M.J., Wei, Q., Qiang, X.K., Xiao, G.Q., 2013b. New evidence for early presence of hominids in North China. Sci. Rep. 3, 2403, doi: 10.1038/srep02403.

Ao, H., Dekkers, M.J., Xiao, G.Q., Yang, X.Q., Qin, L., Liu, X.D., Qiang, X.K., Chang, H., Zhao, H., 2012. Different orbital rhythms in the Asian summer monsoon records from North and South China during the Pleistocene. Global Planet. Change 80-81, 51-60.

Ao, H., Deng, C.L., Dekkers, M.J., Liu, Q.S., Qin, L., Xiao, G.Q., Chang, H., 2010a. Astronomical dating of the Xiantai, Donggutuo and Maliang Paleolithic sites in the Nihewan Basin (North China) and implications for early human evolution in East Asia. Palaeogeogr. Palaeoclimatol. Palaeocl. 297, 129-137.

Ao, H., Deng, C.L., Dekkers, M.J., Sun, Y.B., Liu, Q.S., Zhu, R.X., 2010b. Pleistocene environmental evolution in the Nihewan Basin and implication for early human colonization of North China. Quat. Int. 223-224, 472-478.

Barbour, G.B., 1925. The deposits of the Sangkanho Valley. Bull. Geol. Soc. China.

4, 53-55

Barbour, G.B., Licent, E., Teilhard de Chardin, P., 1927. Geological study of the deposits of the Sangkanho Basin. Bull. Geol. Soc. China. 5, 263-278

Berger, A., Loutre, M. F., 1991. Insolation values for the climate of the last 10 million years. Quat. Sci. Rev. 10, 297–317.

Berger, W.H., Jansen, E., 1994. Mid-Pleistocene climate shift - the Nansen Connection. In: Johannessen, O.M., Muench, R.D., Overland, J.E. (Eds.), The Polar Oceans and Their Role in Shaping the Global Environment, Geophysical Monograph Series, vol. 84. American Geophysical Union, pp. 295-311.

Braun, D.R., Norton, C.J., Harris, J.W.K., 2010. Africa and Asia: comparisons of the earliest archaeological evidence. In: Norton, C.J., Braun, D.R., (Eds.), Asian Paleoanthropology: From Africa to China and Beyond. Vertebrate Paleobiology and Paleoanthropology, Springer Science + Business Media B.V. 41-48.

Cai, B. Q., Zheng, S. H., Liddicoat, J. C., Li, Q., 2013. Review of the Litho-, Bio-, and Chronostratigraphy in the Nihewan Basin, Hebei, China. In: Wang, X. M., Flynn, L. J., Fortelius, M., eds, Fossils of Asia: Neogene biostratigraphy and Chronology. New York: Columbia University Press, 218-242.

Chen, C., Shen, C., Chen, W., Tang, Y. J., 2002. Lithic analysis of the Xiaochangliang industry. Acta Anthropol. Sin. 21, 23-40.

Clark, P.U., Archer, D., Pollard, D., Blum, J.D., Rial, J.A., Brovkin, V., et al. 2006. The Middle Pleistocene transition: Characteristics, mechanisms, and implications for long-term changes in atmospheric pCO_2. Quat. Sci. Rev. 25(23-24), 3150-3184.

de la Torre, I., Mora, R., 2018. Oldowan technological behaviour at HWK EE (Olduvai Gorge, Tanzania). J. Hum.Evol. 120, 236-273.

Deng, C. L., Hao, Q. Z., Guo, Z. T., Zhu, R. X., 2019. Quaternary integrative stratigraphy and timescale of China. Science China Earth Sciences, 62(1), 324-348, doi:10.1007/ s11430-017-9195-4.

Deng, C. L., Shaw, J., Liu, Q. S., Pan, Y. X., Zhu, R. X., 2006a. Mineral magnetic variation of the Jingbian loess/paleosol sequence in the northern Loess Plateau of China: Implications for Quaternary development of Asian aridification and cooling. Earth Planet. Sci. Lett. 241, 248-259.

Deng, C. L., Wei, Q., Zhu, R. X., Wang, H. Q., Zhang, R., Ao, H., Chang, L., Pan, Y. X., 2006b. Magnetostratigraphic age of the Xiantai Paleolithic site in the Nihewan Basin and implications for early human colonization of Northeast Asia. Earth Planet. Sci. Lett. 244, 336-348.

Deng, C. L., Xie, F., Liu, C. C., Ao, H., Pan, Y. X., Zhu, R. X., 2007. Magnetochronology of the Feiliang Paleolithic site in the Nihewan Basin and implications for early human adaptability to high northern latitudes in East Asia. Geophys. Res. Lett. 34, L14301. doi: 14310.11029/ 12007GL030335.

Deng, C. L., Zhu, R. X., Zhang, R., Ao, H., Pan, Y. X., 2008. Timing of the Nihewan formation and faunas. Quat. Res. 69, 77-90.

Dennell, R.W., 2009. The Palaeolithic Settlement of Asia. Cambridge University Press, Cambridge.

Dennell, R., 2010. “Out of Africa I”: Current Problems and Future Prospects. In: Fleagle, J.G., et al. (eds.), Out of Africa I: The First Hominin Colonization of Eurasia, Vertebrate Paleobiology and Paleoanthropology, Springer Science+Business Media B.V. 247-273.

Dennell, R. W., 2013. The Nihewan Basin of North China in the Early Pleistocene: continuous and flourishing, or discontinuous, infrequent and ephemeral occupation? Quat. Int. 295, 223-236.

Dennell, R., Roebroeks, W., 2005. An Asian perspective on early human dispersal from Africa. Nature 438, 1099-1104.

Ding, Z. L., Derbyshire, E., Yang, S. L., Yu, Z. W., Xiong, S. F., Liu, T. S., 2002. Stacked 2.6-Ma grain size record from the Chinese loess based on five sections and correlation with the deep-sea $\delta^{18}O$ record. Paleoceanography 17, 1033, doi: 10.1029/2001PA000725.

Ding, Z. L., Derbyshire, E., Yang, S. L., Sun, J. M., Liu, T. S., 2005. Stepwise expansion of desert environment across northern China in the past 3.5 Ma and implications for monsoon evolution. Earth Planet. Sci. Lett. 237, 45-55.

Ferring, R., Omsb, O., Agustíc, J., Berna, F., Nioradze, M., Shelia, T., Tappen, M., Vekua, A., Zhvania, D., Lordkipanidze, D., 2011. Earliest human occupations at Dmanisi (Georgian Caucasus) dated to 1.85–1.78 Ma. Proc. Natl. Acad. Sci. USA 108, 10432-10436.

Gabunia L, Vekua A. 1995. A Plio-Pleistocene hominid from Dmanisi, East Georgia, Caucasus. Nature 373, 509-512.

Gabunia, L., Vekua, A., Lordkipanidze, D. Swisher, C. C., Ferring, R., Justus, A., Nioradze, M., Tvalchrelidze, M., Antón, S.C., Bosinski, G., Joris, O., de Lumley, M.A., Majsuradze, G., Mouskhelishvili, A., 2000. Earliest Pleistocene hominid cranial remains from Dmanisi, Republic of Georgia: taxonomy, geological setting, and age. Science 288, 1019-1025.

Gao, X., Norton, C.J., 2002. Critique of the Chinese "Middle Paleolithic". Antiquity 76, 397-412.

Gao, X., Wei, Q., Shen, C., Keates, S., 2005. New light on the earliest hominid occupation in East Asia. Curr. Anthropol. 46, s115-s120.

Guan, Y., Wang, F. G., Xie, F., Pei, S. W., Zhou, Z. Y., Gao, X., 2016. Flint knapping strategies at Cenjiawan, an Early Paleolithic site in the Nihewan Basin, North China. Quat. Int. 400, 86-92.

Head, M. J., Gibbard, P. L., 2015. Early-Middle Pleistocene transitions: Linking terrestrial and marine realms. Quat. Int. 389, 7-46.

Head, M.J., Pillans, B., Farquhar, S., 2008. The Early-Middle Pleistocene Transition: characterization and proposed guide for the defining boundary. Episodes 31(2), 255-259.

Henke, W., Hardt, T., 2011. The Genus *Homo*: Origin, Speciation and Dispersal. In:

Condemi, S., and Weniger, G.C. (eds.), Continuity and Discontinuity in the Peopling of Europe: One Hundred Fifty Years of Neanderthal Study. Vertebrate Paleobiology and Paleoanthropology, Springer Science+ Business Media B.V. 17-45.

Hilgen, F. J., Lourens, L. J. & van Dam, J. A. The Neogene Period. In: The Geologic Time Scale 2012 (eds. Gradstein, F., Ogg, J. G., Schmitz, M. D. & Ogg, G. M.) 923-978 (Elsevier, 2012).

Isaac, G. Ll., 1986. Foundation stones: early artifacts as indicators of activities and abilities. In: G, N. Bailey and P.Callow (eds). Stone Age Prehistory-studies in memory of Charles Mcburney. Cambridge: Cambridge University Press, pp. 221-241.

Isaac, G. Ll., Harris, J. W. K., Marshall, F., 1981. Small is informative: the application of the study of mini-sites and least effort criteria in the interpretation of the Early Pleistocene archaeological record at Koobi Fora, Kenya. Proc. Union Internacional de Ciencias Prehistoricas Y Protohistoricas; X Congress, Mexico City. Mexico, pp. 101–119.

Keates, S.G., 2000. Early and Middle Pleistocene Hominid Behavior in Northern China. BAR International Series 863. John and Hedges, Oxford, p. 107.

Keates, S. G., 2010. Evidence for the earliest Pleistocene hominid activity in the Nihewan Basin of northern China. Quat. Int. 223-224, 408-417.

King, J. W., Channell, J. E. T., 1991. Sedimentary magnetism, environmental magnetism, and magnetostratigraphy. Rev. Geophys. 29, 358-370.

Kirschvink, J.L., 1980. The least-squares line and plane and the analysis of palaeomagnetic data. Geophys. J. R. Astron. Soc. 62, 699–718.

Klein, R., 2009. Hominin dispersals in the old world. In: Scarre, C., ed. The Human Past-world prehistory and development of human societys (2nd edition). London: Thames & Hudson, 84-123.

Kleindienst, M.R., 1962. Component of the East African Acheulian assemblage: An analytic approach. In: Mortelmans, G., Nenquin, J. (Eds.), Actes du IV Congrés Panafricain de Préhistoire et de l'Etude du Quaternaire, Leopoldville, 1959. Tervuren, Belgie Annalen, Musée Royal de l'Afrique Centrale, Tervuren, 81-108.

Larick, R., Ciochon, R. L., 1996. The African emergence and early Asian dispersals of the genus *Homo*. Am. Sci. 84(6), 538-551.

Li, X. L., Pei, S. W., Jia, Z. X., Guan, Y., Niu, D. W., Ao, H., 2016. Paleo-environmental conditions at Madigou (MDG), a newly discovered Early Paleolithic site in the Nihewan Basin, North China. Quat. Int. 400, 100-110.

Li, Y. X., 1999. On the progressiveness of the stone artifacts from the Xiaochangliang site at Yangyuan, Hebei. Acta Anthropol. Sin. 18(4), 241-254.

Liu, L. Q., Wang, F. G., Yang, S. X., Yue, J. P., 2018. A preliminary report on the stone artifacts of 2016 excavation of Maliang Locality 10 in the Nihewan Basin. Acta Anthropol. Sin. 37(3), 419-427.

Liu, P., Deng, C. L., Li, S. H., Cai, S. H., Cheng, H. J., Yuan, B. Y., Wei, Q., Zhu,

R. X., 2012. Magnetostratigraphic dating of the Xiashagou Fauna and implication for sequencing the mammalian faunas in the Nihewan Basin, North China. Palaeogeogr. Palaeoclimatol. Palaeocl. 315-316, 75-85.

Liu, P., Deng, C. L., Li, S. H., Zhu, R. X., 2010. Magnetostratigraphic dating of the Huojiadi Paleolithic Site in the Nihewan Basin, North China. Palaeogeogr. Palaeoclimatol. Palaeocl. 298, 399-408.

Liu, P., Yue, F., Liu, J. Q., Qin, H. F., Li, S. H., Zhao, X., Xu. J. W., Yuan, B. Y., Deng, C. L., Zhu, R. X., 2018. Magnetostratigraphic dating of the Shixia red sediments and implications for formation of Nihewan paleo-lake, North China. Quat. Sci. Rev. 193, 118-128.

Liu, Y., Hou, Y. M., Ao, H., 2013. Analysis of lithic technology of Lower Pleistocene sites and environmental information in the Nihewan bain, North China. Quat. Int. 295, 215-222.

Maasch, K.A., 1988. Statistical detection of the mid-Pleistocene transition. Clim. Dynam. 2, 133-143.

Medina-Elizalde, M., Lea, D. W., 2005. The mid-Pleistocene transition in the tropical Pacific. Science 310, 1009-1012.

Min, L. R., Chi, Z. Q., 2003. Quaternary Geology of the Western Yangyuan Basin (in Chinese with English abstract). Geological Publishing House, Beijing.

Mudelsee M, Schulz M. 1997. The Mid-Pleistocene climate transition: Onset of 100 ka cycle lags ice volume build-up by 280 ka. Earth Planet. Sci. Lett. 1997, 151(1), 117-123.

Norton, C. J., Braun, D. B., 2010. Asian paleoanthropology: an introduction. In: C. J. Norton and D. B. Braun (eds), Asian Paleoanthropology: From Afriva to China and Beyond, Vertebrate Paleobiology and paleoanthropology. Springer Science+Business Media B. V. 1-4.

Parfitt, S.A., Ashton, N.M., Lewis, S.G., Abel, R.L., Coope, G.R., Field, M.H., Gale, R., Hoare, P.G., Larkin, N.R., Lewis, M.D., Karloukovski, V., Maher, B.A., Peglar, S.M., Preece, R.C., Whittaker, J.E., Stringer, C.B., 2010. Early Pleistocene human occupation at the edge of the boreal zone in northwest Europe. Nature 466, 229-233.

Pei, S. W., Ma, N., Li, X.L., 2010. A report on the discovery of some Paleolithic localities on the eastern part of Nihewan Basin in 2007. Acta Anthropol. Sin. 29, 33-43 (in Chinese).

Pei, S. W., Xie, F., Deng, C. L., Jia, Z. X., Wang, X. M., Guan, Y., Li, X. L., Ma, D. D., de la Torre, I., 2017. Early Pleistocene archaeological occurrences at the Feiliang site, and the archaeology of human origins in the Nihewan Basin, North China. Plos One, 12(11): e0187251.

Potts, R., 1996. Evolution and climate variability. Science, 273, 922-923.

Potts, R., 1998. Environmental hypotheses of hominin evolution. Yearb. Phys. Anthropol. 41, 93-136.

Potts, R., 2001. Mid-Pleistocene environmental change and human evolution, in Human Roots: Africa and Asia in the Middle Pleistocene, edited by L. Barham and K. Robson-Brown, pp. 5–21, West. Acad. and Spec. Press

Ltd., Bristol, U.K.

Potts, R., Teague, R., 2010. Behavioral and environmental background to 'Out-of-Africa I' and the arrival of *Homo erectus* in East Asia. In: J.G. Fleagle, J.J. Shea, F.E. Grine, A.L. Baden, & R.E. Leakey (Eds.), Out of Africa I: the first hominin colonization of Eurasia. Dordrecht: Springer, 67–85.

Potts, R., 2012. Evolution and environmental change in early human prehistory. Annu. Rev. Anthropol. 41, 151–167.

Potts, R. 2013. Hominin evolution in setting of strong environmental variability. Quat. Sci. Rev. 73: 1-13.

Qiu, Z.X., 2000. Nihewan fauna and Q/N boundary in China. Quat. Sci., 20: 142-154 (in Chinese).

Raymo, M. E., Oppo, D.W., Curry, W., 1997. The mid-Pleistocene climate transition: A deep sea carbon isotopic perspective. Paleoceanography, 12, 546– 559.

Roberts, A. P., Cui, Y., Verosub, K. L., 1995. Wasp-waisted hysteresis loops: mineral magnetic characteristics and discrimination of components in mixed magnetic systems. J. Geophys. Res. 100, 17909–17924.

Ruddiman, W.F., Raymo, M., McIntyre, A., 1986. Matuyama 41,000-year cycles: North Atlantic Ocean and northern hemisphere ice sheets. Earth Planet. Sci. Lett. 80, 117-129.

Schick, K.D., 1994. The Movius line reconsidered: Perspectives on the Earlier

Paleolithic of Eastern Asia, in: Corruccini, R., Ciochon, R. (Eds.), Integrative Paths to the Past: Paleoanthropological Advances in Honor of F. Clark Howell. Prentice Hall, Englewood Cliffs, pp. 569-596.

Schick, K.D., Dong, Z., 1993. Early Paleolithic of China and Eastern Asia. Evol. Anthropol. 2, 22-35.

Schick, K., Toth, N., Wei, Q., Clark, J. D., Etler, D., 1991. Archaeological perspectives in the Nihewan Basin, China. J. Hum. Evol. 21, 13-26.

Shen, C., Chen, C., 2003. New evidence of Hominid behavior from Xiaochangliang, Northern China: site formation and lithic technology. In: Shen, C., and Keates, S., eds, Current Research in Chinese Pleistocene Archaeology. BAR International Series 1179, 67-82.

Shen, C., Wei, Q., 2004. Lithic Technological vaviability of the Middle Pleistocene in the eastern Nihewan Basin, North China. Asian Perspectives 43, 281-301.

Stacey, F. D., Banerjee, S. K., 1974. The Physical Principles of Rock Magnetism. (Elsevier, 1974).

Sun, Y. B., Yin, Q. Z., Crucifix, M., Clemens, S. C., Araya-Melo, P., Liu, W. G., Qiang, X. K., Liu, Q. S., Zhao, H., Liang, L. J., Chen, H. Y., Li, Y., Zhang, L., Dong, G. C., Li, M., Zhou, W. J., Berger, A., An, Z. S., 2019. Diverse manifestations of the mid-Pleistocene climate transition. Nat. Commun. 10: 352, https://doi.org/10.1038/s41467-018- 08257-9.

Teilhard de Chardin, P., Piveteau, J., 1930. Les mammiferes fossils de Nihowan (Chine). Annales de Paleontologie, 19, 1-154.

Tian, J., Wang, P., Cheng, X., Li, Q.,2002. Astronomically tuned Plio–Pleistocene benthic $\delta^{18}O$ record from South China Sea and Atlantic–Pacific comparison. Earth Planet. Sci. Lett. 203, 1015−1029.

Vallverdú, J., Saladié, P., Rosas, A., Huguet, R., Cáceres, I., Mosquera, M., Garcia-Tabernero, A., Estalrrich, A., Lozano-Fernández, I., Pineda-Alcalá, A., Carrancho, Á., Villalaín, J.J., Bourlès, D., Braucher, R., Lebatard, A., Vilalta, J., Esteban-Nadal, M., Bennàsar, M.L., Bastir, M., López-Polín, L., Ollé, A., Vergés, J.M., Ros-Montoya, S., Martínez-Navarro, B., García, A., Martinell, J., Expósito, I., Burjachs, F., Agustí, J., Carbonell, E., 2014. Age and Date for Early Arrival of the Acheulian in Europe (Barranc de la Boella, la Canonja, Spain). PLoS ONE 9(7), e103634.

Wang, H.Q., Deng, C.L., Zhu, R.X., Wei, Q., Hou, Y.M., Boeda, E., 2005. Magnetostratigraphic dating of the Donggutuo and Maliang Paleolithic sites in the Nihewan Basin, North China. Quat. Res. 64, 1-11.

Wang, H.Q., Deng, C.L., Zhu, R.X., Xie, F., 2006. Paleomagnetic dating of the Cenjiawan Paleolithic site in the Nihewan Basin, northern China. Science in China 49, 295-303.

Wei, Q., 1985. Palaeoliths from the Lower Pleistocene of the Nihewan beds in the Donggutuo site. Acta Anthropol. Sin. 4, 289-330.

Wei, Q., Xie, F., 1989. Selected treatises on Nihewan. Beijing: Cultural relics Publishing House (in Chinese).

Winder, I. C., Devés, M. H., King G. C. P., Bailey, G. N., Inglis, R. H., Meredith-Williams, M., 2015. Evolution and dispersal of the genus Homo: A landscape approach. J. Hum. Evol. 87, 48-65.

Xie, F., Toth, N., Schick. K., Clark, D. J., 1994. The refitting study of Cenjiawan lithic artifacts unearthed in 1986. J. Chinese Antiq. 3, 86–102.

Xie, F., Li, J., Liu, L.Q., 2006. Paleolithic Archaeology in the Nihewan Basin (in Chinese). Huashan Literature & Arts Press, Shijiazhuang, China, pp. 278.

Yang, S. X., Hou, Y. M., Yue, J. P., Petraglia, M. D., Deng, C. L., Zhu, R. X., 2016. The lithic assemblages of Xiaochangliang, Nihewan Basin: Implications for Early Pleistocene hominin behaviour in North China. PLoS ONE 11(5), e0155793.

Yang, S. X., Petraglia, M. D., Hou, Y. M., Yue, J. P., Deng, C. L., Zhu, R. X., 2017. The lithic assemblages of Donggutuo, Nihewan Basin: Knapping skills of Early Pleistocene hominins in North China. PLoS ONE 12(9), e0185101.

You, Y., Tang, Y. J., Li, Y., 1980. Paleolithic discoveries in the Nihewan formations. Chinese Quat. Res. 5, 1-13. (In Chinese with English abstract)

Young, C. C., 1950. The Plio-Pleistocene boundary in China. In: Report on 18th International Geological Congress, London, 115-125.

Yuan, B. Y., Xia, Z. K., Niu, P. S., 2011. Nihewan Rift and Paleoanthropology. Beijing: Geological Publishing House (in Chinese with English Abstract).

Zhou, T. R., Li, H. Z., Liu, Q. S., Li, R. Q., Sun, X. P., 1991.Study on the Cenozoic paleogeograpgy of Nihewan Basin. Beijing: Science Press, 1-162 (in Chinese).

Zhu, R. X., Hoffman, K. A., Potts, R., Deng, C. L., Pan, Y. X., Guo, B., Shi, C. D., Guo, Z. T., Yuan, B. Y., Hou, Y. M., Huang, W. W., 2001. Earliest presence of humans in northeast Asia. Nature 413, 413-417.

Zhu, R. X., An, Z. S., Potts, R., Hoffman, K. A., 2003. Magnetostratigraphic dating of early humans in China. Earth Sci. Rev. 61, 341–359.

Zhu, R. X., Potts, R., Xie, F., Hoffman, K. A., Deng, C. L., Shi, C. D., Pan, Y. X., Wang, H. Q., Shi, R. P., Wang, Y. C., Shi, G. H., Wu, N. Q., 2004. New evidence on the earliest human presence at high northern latitudes in Northeast Asia. Nature 431, 559-562.

Zhu, R. X., Potts, R., Pan, Y. X., Yao, H. T., Lü, L. Q., Zhao, X., Gao, X., Chen, L. W., Gao, F., Deng, C. L., 2008. Early evidence of the genus *Homo* in East Asia. J. Hum. Evol. 55, 1075-1085.

Zhu, Z. Y., Dennell, R., Huang, W. W., Wu, Y., Rao, Z. G., Qiu, S. F., Xie, J. B., Liu, W., Fu, S. Q., Han, J. W., Zhou, H. Y., Yang, T. P. O., Li, H. M., 2015. New dating of the *Homo erectus* cranium from Lantian (Gongwangling), China. J. Hum. Evol. 78, 144-157.

Zhu, Z. Y., Dennell, R., Huang, W. W., Wu, Y., Qiu, S. F., Yang, S. X., Rao, Z. G., Hou, Y. M., Xie, J. B., Han, J. W., Ouyang, T. P., 2018. Hominin occupation of the Chinese Loess Plateau since about 2.1 million years ago. Nature 599, 608-612.

Zijderveld, J. D. A., 1967. A.C. demagnetization of rocks: analysis of results. In: Collinson, D. W., Creer, K. M., Runcorn, S. K. (Eds.), Methods in Paleomagnetism. Elsevier, New York, pp. 254–286.

Zuo, T. W., Cheng, H. J., Liu, P., Xie, F., Deng, C. L., 2011. Magnetostratigraphic dating of the Hougou Paleolithic site in the Nihewan Basin, North China. Sci. China Earth Sci. 54, 1643-1650.